

Correlation of Dermatoscopic Findings in Leprosy with Clinical Spectrum and Histopathology: A Prospective Observational Study

Sameeha HC¹, Sravani K², Divya B³, Panati M⁴, D Indira⁵, SK Manjunath⁶, A Venkata Krishna⁷, T Rajeev Singh⁸

Received: 27.04.2024

Revised: 31.05.2024

Accepted: 23.06.2024

The variety of clinical presentations makes leprosy a diagnostic challenge and it must be differentiated from other granulomatous dermatoses. Dermoscopy is a handy tool that can aid in its diagnosis. This study has been carried out to evaluate the dermoscopic findings in different spectrums of leprosy and its reactions and to correlate it with the clinical and histopathological findings. This was a prospective observational study of treatment naïve leprosy patients carried out over a period of 6 months. The study patients were categorized as per Ridley-Jopling classification. Dermoscopy and biopsy of every patient were carried out. A total of 50 patients were recruited in this study. The most common type of leprosy found was Lepromatous Leprosy (30%), followed by Borderline Tuberculoid leprosy (22%). Type 1 lepra reaction was noted in 13 patients, whereas 12 patients exhibited type 2 lepra reactions. White and yellowish brown structureless areas histologically corresponding to dermal granulomas, whereas chrysalis-like streaks and variable loss of appendageal structures, corresponding to dermal fibrosis and peri appendageal granulomas, respectively were the predominant features. Scaling, yellowish brown structureless areas, reduced pigmentary network were more commonly seen towards tuberculoid pole whereas accentuation of reticular pigment and chrysalis like streaks towards the lepromatous pole. Erythema, dilated blood vessels were seen in patients in reaction meanwhile follicular plugging and scaling were observed in type 1 reaction. Other unique findings included targetoid pattern and petal like arrangement in type 2 reaction and Histoid Hansens, respectively. The data showed an excellent correlation between histology and dermoscopic findings. Dermoscopy is a non-invasive tool that can complement histopathological tests.

Keywords: Leprosy, Dermoscopy, Histopathology, Granulomatous Disorders, Histoid Hansen, Reactions

Introduction

Leprosy is a chronic granulomatous disorder of the skin and nerves caused by *Mycobacterium*

leprae (Sardana 2020). Various classifications have been used for leprosy with Ridley-Jopling classification being the most broadly accepted.

¹ Dr Sameeha Hamza Chenganasseri, MD, Senior Resident, Orcid ID: 0000-0002-1394-1331

² Dr Sravani Kapilavayi, MD, Assistant Professor

³ Dr Badavath Divya, Postgraduate, Orcid ID: 0009-0005-0056-5997

⁴ Dr Malini Panati, MD, Associate Professor

⁵ Dr D Indira, MD, Associate Professor, Orcid ID : 0000-0002-9563-9290

⁶ Dr Manjunatha SK, MD, Consultant Dermatologist

⁷ Dr A Venkata Krishna, MD, Professor

⁸ Dr T Rajeev Singh, Professor and Head of Department, Orcid ID: 0000-0002-8172-3678

Department of Dermatology, Venereology and Leprosy, Osmania Medical College, Hyderabad-500095, Telangana, India

Corresponding Author: Dr Badavath Divya; **Email:** drdivyabadavath@gmail.com

According to Ridley-Jopling classification (Ridley & Jopling 1966), patients are classified into tuberculoid leprosy (TT), borderline tuberculoid (BT) leprosy, mid-borderline (BB) leprosy, borderline lepromatous (BL) leprosy, and lepromatous leprosy (LL) based on clinical, immunological, and pathological features. Indeterminate Hansen has been described in the Indian Association of Leprologists classification (IAL 1982, Sardana 2020).

Leprosy reactions are acute immunological phenomenon superimposed on the otherwise chronic course of leprosy. Two distinct types of leprosy reaction can occur: Type 1 reactions and Type 2 reactions. Type 1 reaction is a delayed hypersensitivity reaction characterized by heightened inflammation in existing lesions and impaired neural function. The type 2 lepra reaction, or erythema nodosum leprosum, manifests as evanescent, tender, superficial and deep erythematous papules and nodules with systemic characteristics (Kar & Gupta 2016).

The clinical manifestations of leprosy can be inconspicuous or obvious depending on the individual's immune status. The vast difference in how leprosy affects people makes it difficult for early diagnosis and treatment. Invasive procedures like slit skin smear and a skin biopsy become necessary for physicians in these situations.

Dermoscopy, also referred to as dermatoscopy, skin surface microscopy, or epiluminescence microscopy, is a non-invasive, in vivo, repeatable, recordable bedside investigation that has long proved helpful in the assessment of doubtful skin lesions. A dermatoscope simulates the function of a magnifying glass and can visualize subsurface skin structures upto the depth of reticular dermis, that are typically invisible to the unaided eye (Sonthalia et al 2019). By confirming the clinical diagnosis using dermoscopic patterns, a skin biopsy can often be avoided. Although

skin biopsy, clinicopathological correlation and slit skin smear are gold standard in confirming the diagnosis, identifying distinct dermoscopic patterns can guide clinicians to consider leprosy as a differential and thus avoid any treatment delay. Recently this approach has been explored by several clinicians working on leprosy (Acharya & Mathur 2020, Agharia et al 2023, Ankada et al 2024, Chopra et al 2019, Jha et al 2020, Mohta et al 2021, Vinay et al 2019). Our study aims at enlarging this emerging experience about clinical applications of dermoscopy in leprosy.

Materials and Methods

This was a prospective observational study of treatment naïve leprosy patients over a period of 6 months. The study was initiated after due approval from the Ethics Board of Osmania Medical College, Hyderabad, Telangana, India and was conducted in the skin outpatient department of Osmania Medical College, Telangana, India for a period of 6 months from July 2022 to December 2022. Patients newly diagnosed as having leprosy or those not started on leprosy treatment were included in the study. Patients with pure neuritic leprosy and not willing to give consent for biopsy were excluded. Written informed consent was obtained from all the patients before their enrolment in the study. A detailed cutaneous and neurological examination was conducted, and patients were categorized based on the Ridley–Jopling classification according to clinical, histopathological, and slit-skin-smear (SSS) results for acid fast bacilli (AFB).

Photographs of the most characteristic lesions on each patient were taken and the lesions were then evaluated by dermoscopy under DermLite DL3N. The noncontact polarized mode was used for visualizing vessel dilatation and scaling. To evaluate appendageal structures like hair follicles and glands, the polarized mode was combined with nonpolarized contact dermoscopy. The same lesion was also later subjected to biopsy

and sent for histopathological examination. Dermoscopic findings were correlated with clinical and histological findings.

Results

A total of 50 leprosy cases were included in our study. The study patients were of Indian ethnicity, with skin phototypes of IV to VI. The number of males (n=30,60%) exceeded the number of females (n=20, 40%). A history of migration was noted in 5 (10%) patients, and a family history of leprosy was positive in 4 (8%) patients. As per Ridley-Jopling's classification, the most common type was lepromatous leprosy (LL) (n=15, 30%) in our study, followed by borderline tuberculoid leprosy (BT) (n=11, 22%), borderline lepromatous leprosy (n=10, 20%), mid-borderline leprosy (n=5, 10%) and tuberculoid leprosy (n=3, 6%). Other atypical clinical types included were indeterminate leprosy (n=3, 6%) and histoid leprosy (n = 3, 6%). Type 1 lepra reaction was noted in 13 patients (26%), whereas 12 patients (24%) exhibited type 2 lepra reactions.

Cases with tuberculoid leprosy presented clinically with single to a few, well-defined, asymmetrical, hypo-aesthetic, erythematous annular plaques (Fig. 1a). On dermoscopic evaluation of the lesions scaling (n=3, 100%), erythema (n=2, 66%), Yellowish brown structureless areas (n=2, 66%), loss of pigment network (n=2, 66%), and reduction of appendages (n=1, 33.3%) were observed (Figs. 1b, c). Histopathological findings revealed well-formed granulomas composed of lymphocytes, epithelioid cells, histiocytes, and occasional giant cells (Fig.1d). Peri-appendageal granuloma and granuloma eroding basal layer were also noted. This correlated with reduction of appendages and loss of pigment network observed.

Patients with borderline tuberculoid leprosy clinically displayed asymmetrical, well-defined, erythematous plaques with satellite lesions (Fig. 2a). On dermoscopy, scaling and white

structureless areas were the most common findings (n=10, 90%), followed by yellowish-brown structureless areas (n=6, 54%), and accentuation of reticular pigment network (n=5, 45%) (Figs. 2b, 2c). Diminished hair follicles and regions with erythematous hues were noted in 3 (27%) and 4 (36%) patients, respectively. The histopathological analysis of borderline tuberculoid lesion displayed an oval granuloma composed of lymphocytes, histiocytes, epithelioid cells, and Langerhans giant cells (Figs. 2d, 2e), correlating with the yellowish brown and white structureless areas noted in dermoscopy. Perivascular and peri-adnexal granulomas, hyperkeratosis, increased melanin in basal layer and dense inflammatory infiltrate in histopathological evaluation correspond to the dermoscopic findings of diminished hair follicles, scaling, accentuation of pigment network and erythematous hue, respectively.

Patients with mid borderline Hansen's (BB) presented with characteristic saucer-shaped plaques with a well-defined inner border and an ill-defined outer border (Fig. 3a). White structureless areas (n=4, 80%), accentuation of the reticular pigment network (n=3, 60%), yellow brown structureless areas (n=3, 60%), and a decrease in appendages (n=2, 40%), were observed on dermoscopic evaluation (Figs. 3b, 3c). Histopathology of the biopsied lesion showed mild hyperkeratosis, increased basal layer pigmentation corresponding to increase in reticular pigment network and dermis showed peri-adnexal and perineural granulomas (Fig. 3d) correlating with observations of sparse appendages and structureless areas.

Multiple, ill-defined, erythematous to hypopigmented macules and plaques were seen clinically in patients with borderline lepromatous leprosy (Fig. 4a). Dermoscopy of borderline lepromatous lesions revealed white chrysalis-like streaks in all patients (n=10, 100%) with

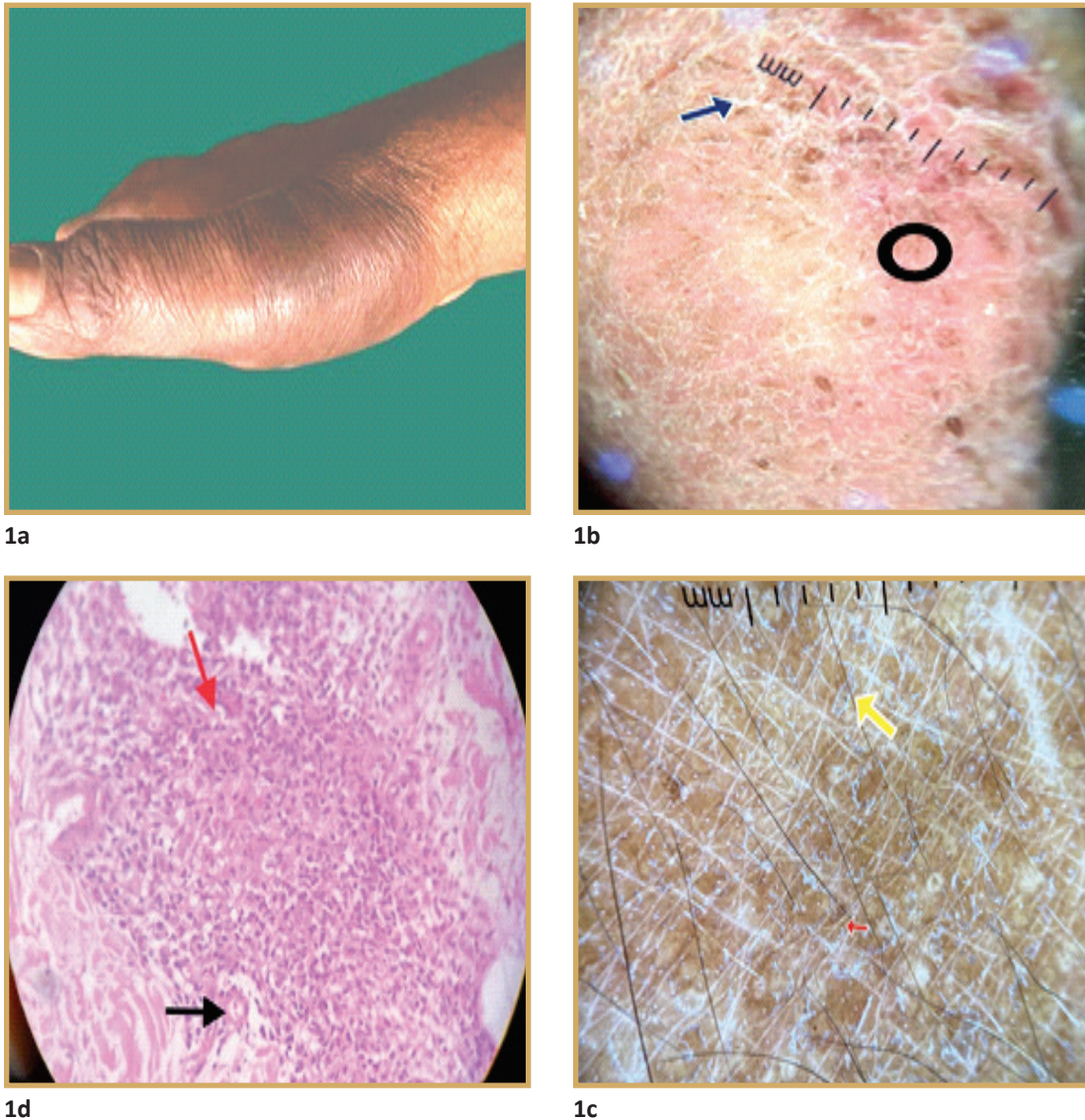


Fig. 1(a-d) : Tuberculoid leprosy. (a) Single, well-defined lesion over dorsum of hand. (b) On dermoscopy of the affected area, scaling (blue arrow) and erythematous hue (black arrow) (DermLite DL3, magnification $\times 10$). (c) Brown structureless areas (red arrow), scaling (yellow arrow) (DermLite DL3, magnification $\times 10$). (d) Histopathology showing well-formed dermal granuloma (red arrow) and perivascular, peri-adnexal and perineural granuloma, composed of lymphocytes, plasma cells, epithelioid, histiocytes, foamy histiocytes, occasional giant cells (black arrow) (H&E, $\times 40$).

accentuation of reticular pigment network (n=9, 90%). Other dermoscopic features included yellowish-brown structureless areas (n=6,

60%), loss of the normal pigment network (n=6, 60%), and scaling (n=4, 40%) (Figs 4b, 4c). The histopathological findings were complementary

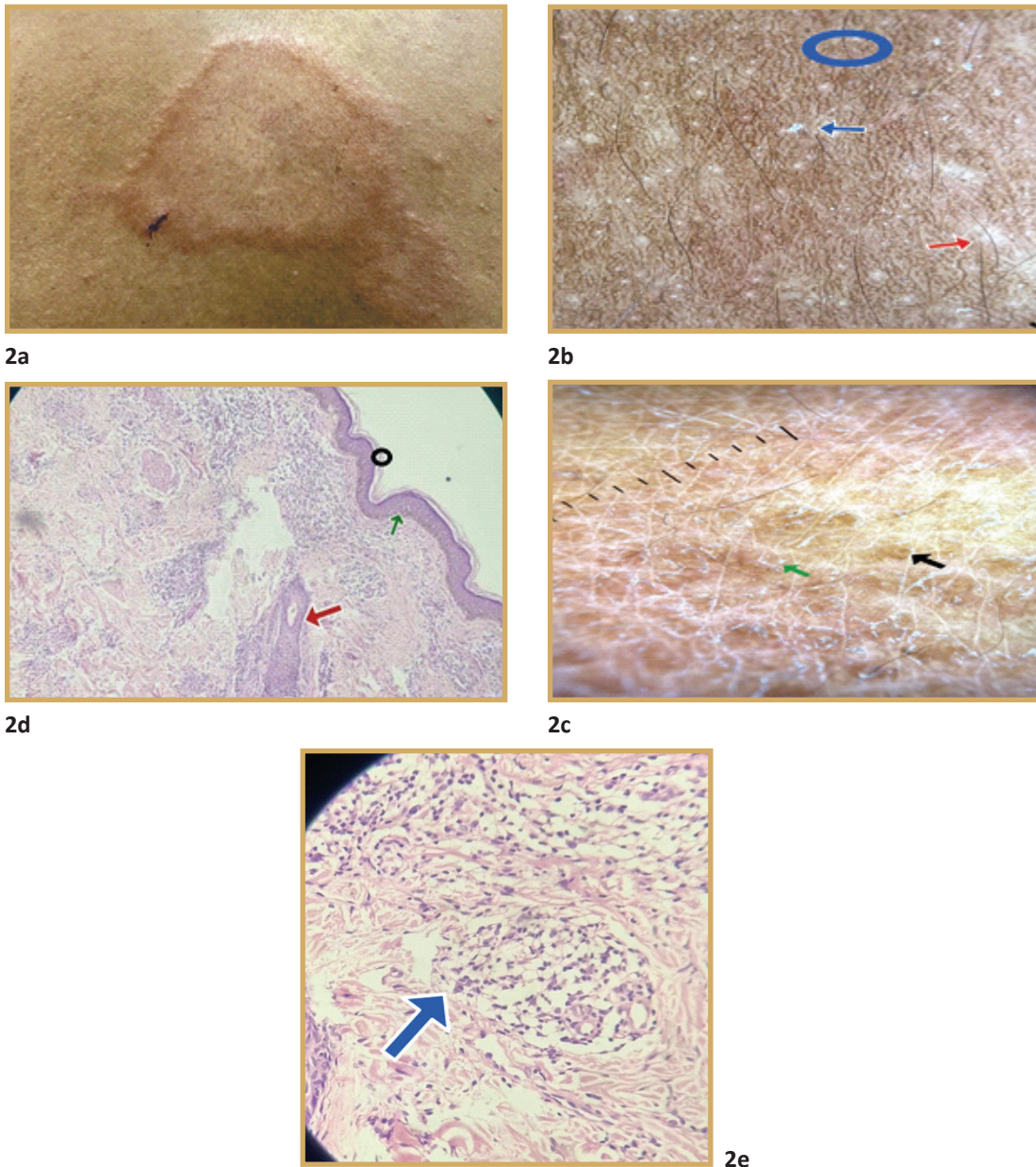
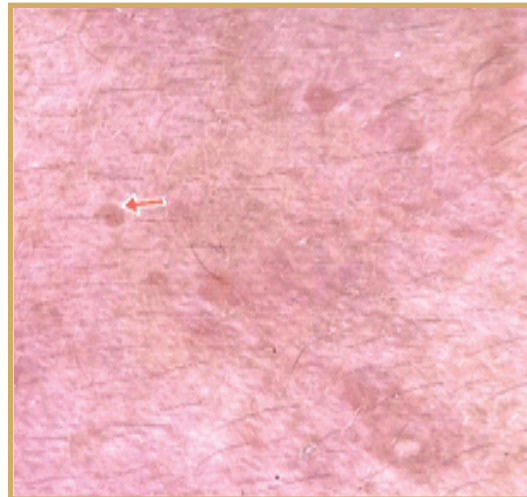


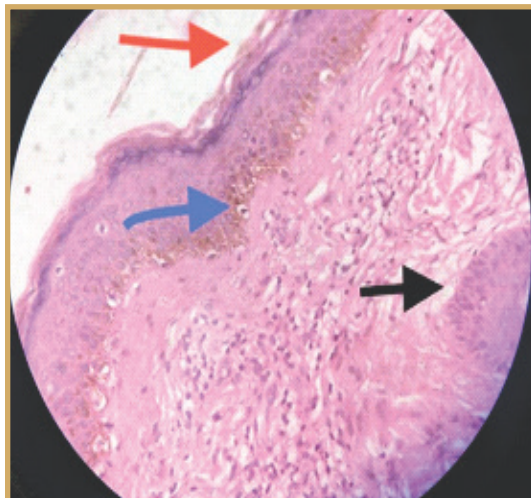
Fig. 2 (a-e): Borderline Tuberculoid Leprosy. (a) well-defined erythematous plaque with central clearing and satellite lesions. **(b)** On dermoscopy of the affected area scaling (blue arrow), diminished hair follicles, white structureless areas (red arrow) and erythematous hue (blue circle) (DermLite DL3, magnification $\times 10$). **(c)** Yellowish brown structureless areas (black arrow) and scaling (green arrow) (DermLite DL3, magnification $\times 10$). **(d)** Histopathology showed hyperkeratosis (black circle), perivascular and peri-adnexal granulomas (red arrow), increased melanin in basal layer (green arrow) and dense inflammatory infiltrate (H&E, $\times 10$). **(e)** Dermal granuloma composed of lymphocytes, histiocytes, epithelioid cells, and Langerhans giant cells (blue arrow) (H&E, $\times 40$).



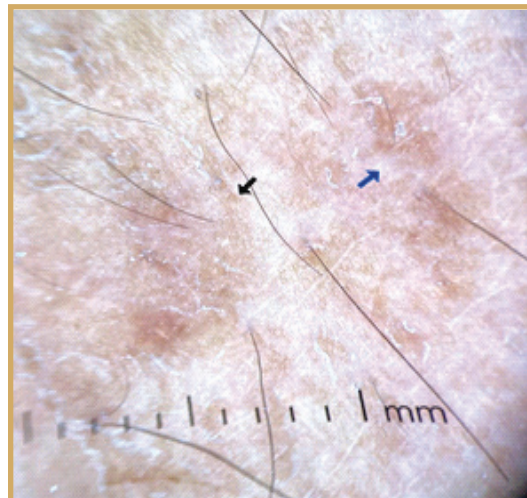
3a



3b



3d



3c

Fig. 3 (a-d) : Borderline borderline (BB) leprosy. (a) Multiple erythematous plaques with punched out appearance with ill-defined outer border and well-defined inner border. (b) On dermoscopy of the affected area yellowish brown structureless areas (red arrow) (DermLite DL3, magnification $\times 10$). (c) Accentuation of reticular pigment network (black arrow), white structureless areas (blue arrow) (DermLite DL3, magnification $\times 10$). (d) Histopathology showing Mild hyperkeratosis (red arrow), increased basal layer pigmentation (blue arrow). Dermis shows peri adnexal and perineural granulomas (black arrow) (H&E, $\times 40$).

to these dermoscopic observations. Loosely formed granulomas composed of foamy macrophages and grenz zone, increased melanin

in basal layer and dermal fibrosis (Figs. 4d, 4e) corresponding to yellowish-brown structureless areas, loss of the normal pigment network, focal

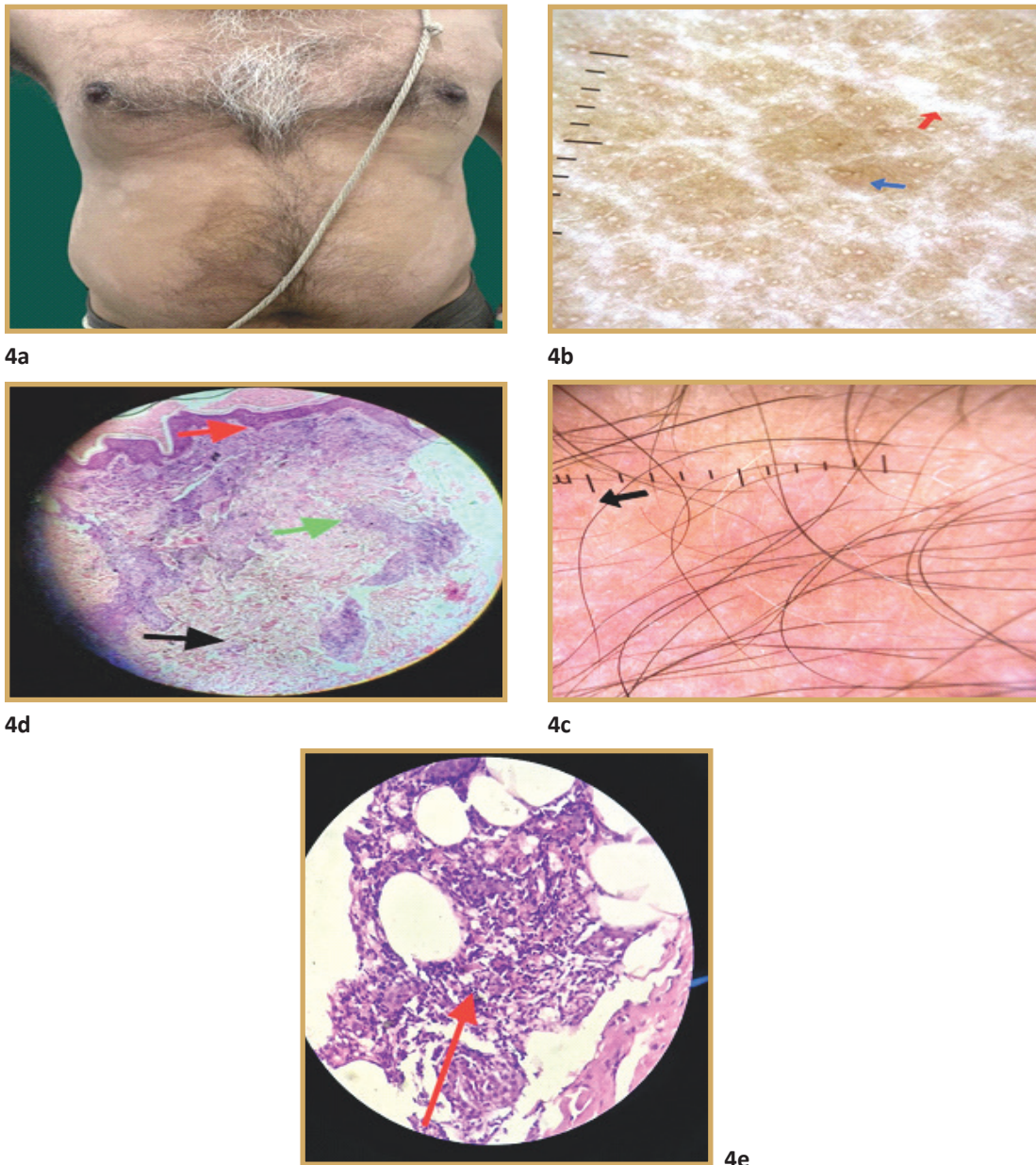


Fig. 4 (a-e): Borderline Lepromatous Leprosy. (a) Multiple, ill -defined, hypopigmented patches. (b) On dermoscopy of the affected area (below the black line), white chrysalis-like structureless areas (red arrow), accentuation of reticular pigment network (blue arrow), loss of hair (DermLite DL3, magnification $\times 10$). (c) Yellowish brown structureless areas (black arrow) (DermLite DL3, magnification $\times 10$). (d) Histopathology showed a loosely formed granulomas composed of foamy macrophages (green arrow) and Grenz zone, increased melanin in basal layer (red arrow) and dermal fibrosis (black arrow) (H&E, $\times 10$). (e) Loosely formed granulomas composed of foamy macrophages and giant cells (red arrow) (H&E, $\times 40$).

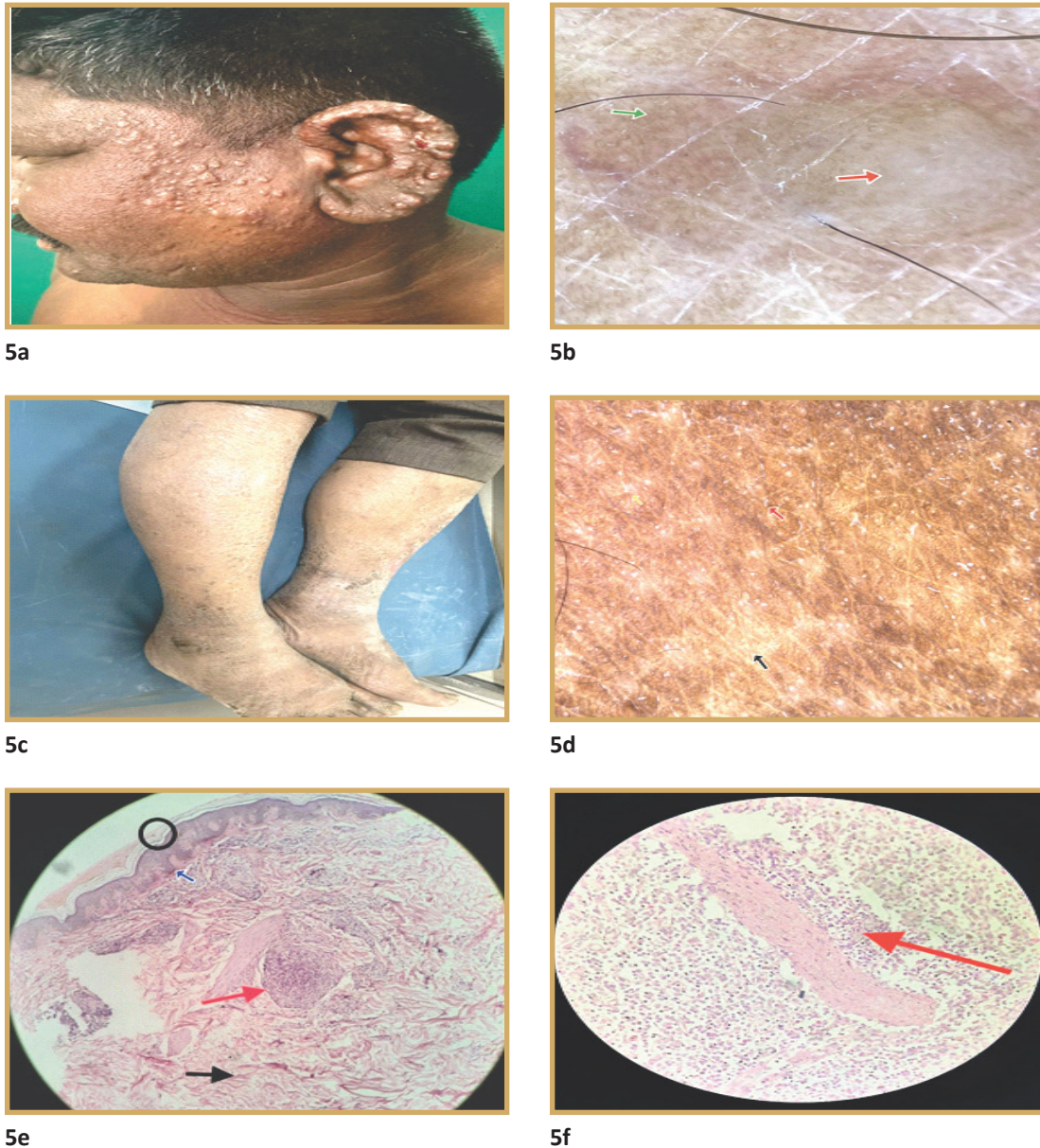


Fig. 5 (a-f): Lepromatous leprosy (LL). (a) Multiple skin-coloured papules and nodules over the infiltrated skin. (b) Ill-defined xerotic patches over bilateral lower limbs. (c) On dermoscopy of papules, central white structureless areas (red arrow) and peripheral accentuation of reticular pigment (green arrow) are noted (DermLite DL3, magnification $\times 10$). (d) Scaling (red arrow), white chrysalis-like structures (black arrow) and erythematous hue (DermLite DL3, magnification $\times 10$). (e) Histopathology showing epidermal hyperkeratosis (black circle), increased melanin in basal layer (blue arrow), numerous granulomas (red arrow), dermal fibrosis (black arrow) (H&E, $\times 10$). (f) Histopathology shows peri-adnexal inflammation (H&E, $\times 40$).

areas of hyperpigmentation, white chrysalis-like structureless areas.

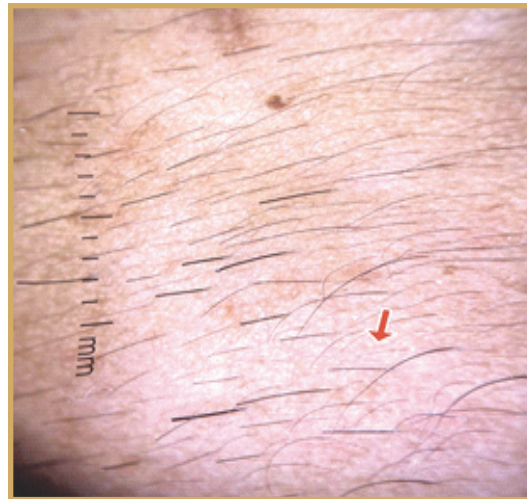
Variable presentations ranging from ill-defined symmetrical hypopigmented macules to nodular and diffuse infiltrative forms were noted in patients with lepromatous leprosy (Figs. 5a, 5b). Accentuation of the normal reticular pigment

network (n=12,80%) and white chrysalis-like structures (n=10, 66.6%) were consistent dermoscopic findings. Xerosis (n=8, 53.3%), yellowish-brown structureless areas (n=6, 40%), and erythematous hues (n=4, 26.6%) were other notable features (Figs. 5c, 5d).

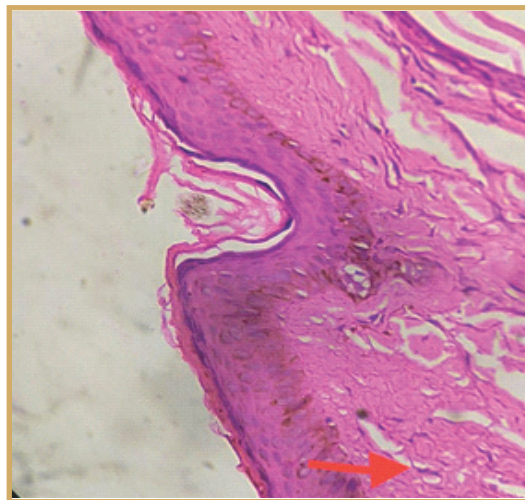
On histopathology, epidermal hyperkeratosis



6a



6b



6c

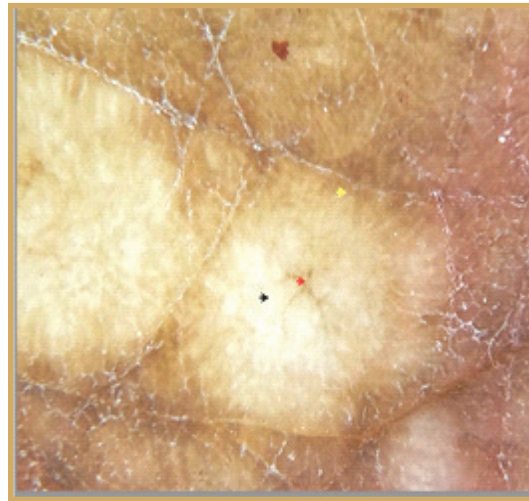
Fig. 6 (a-c): Indeterminate Hansen, (a) single, ill-defined, hypopigmented patch over face. (b) On dermoscopy of the affected area, patchy loss of pigment network (red arrows) (DermLite DL3, magnification $\times 10$). (c) Histopathology showing perivascular and peri-adnexal lymphohistiocytic cells (red arrow) (H&E, $\times 40$)

and ill-defined diffuse granulomatous infiltration with an abundance of foamy macrophages were observed (Fig. 5e) in biopsies from LL

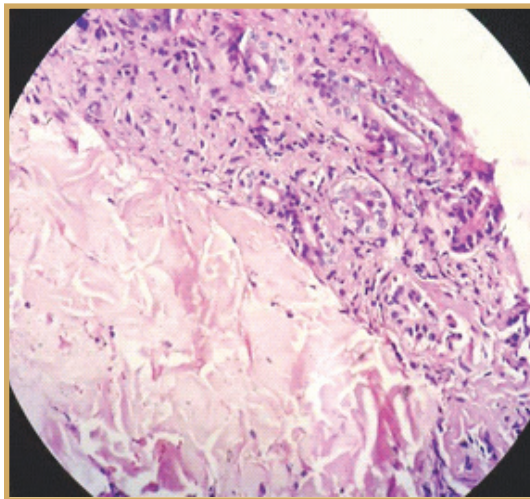
cases. Histopathological findings of epidermal hyperkeratosis, peri-adnexal inflammation (Fig. 5f), numerous granulomas, dermal fibrosis,



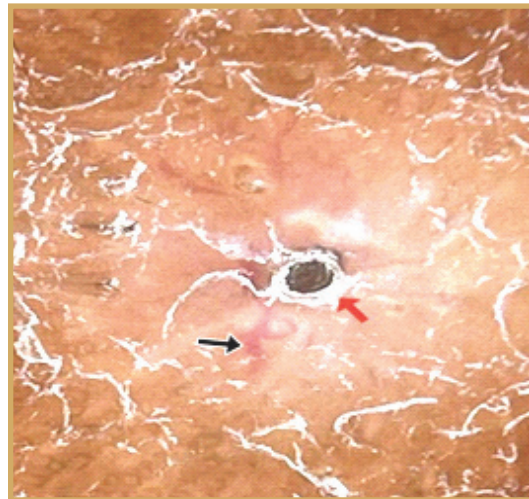
7a



7b



7d



7c

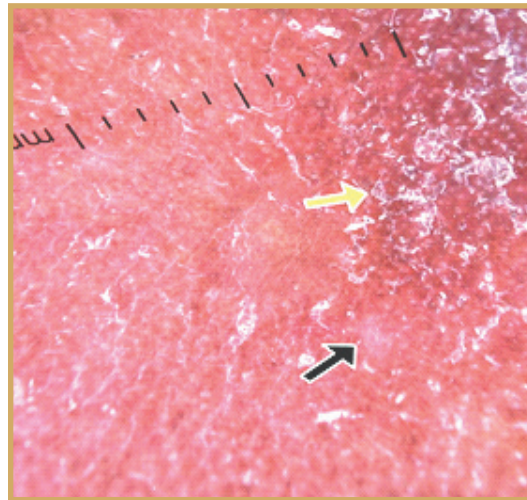
Fig. 7 (a-d): Histoid Hansen. (a) Multiple, flesh-colored, dome-shaped, shiny, succulent nodules with central umbilication. (b) On dermoscopy of the affected area central white structureless areas (black arrow), crown vessel (red arrow), peripheral pigmentation (yellow arrow) (DermLite DL3, magnification $\times 10$). (c) central keratotic plug (red arrow) with crown blood vessels (black arrow), peripheral hyperpigmentation (DermLite DL3, magnification $\times 10$). (d) Histopathology showing a well-formed dermal granuloma with spindle-shaped cells and dermal fibrosis. (H&E, X100)

and increased melanin in the basal layer. These findings can be correlated to scaling, xerosis, yellowish-brown structureless areas, white chrysalis-like structures and accentuation of the

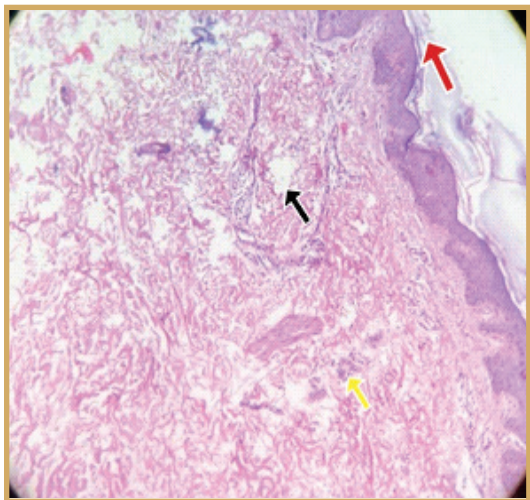
normal reticular pigment network, respectively. Patients with indeterminate Hansens (Fig. 6a) presented with a single, ill-defined, scaly, hypopigmented patch. Dermoscopic



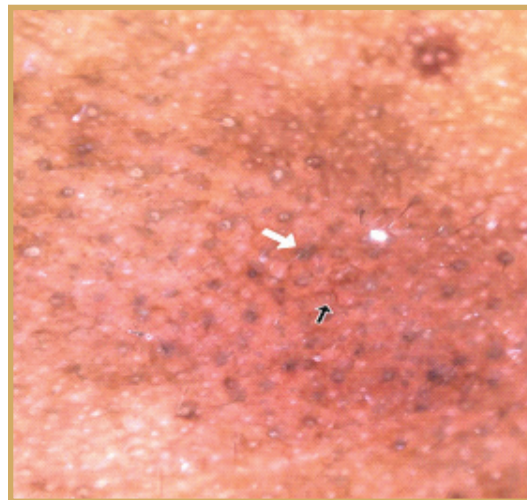
8a



8b



8d

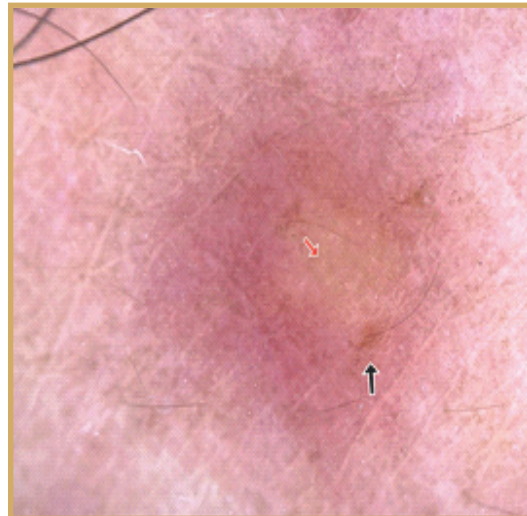


8c

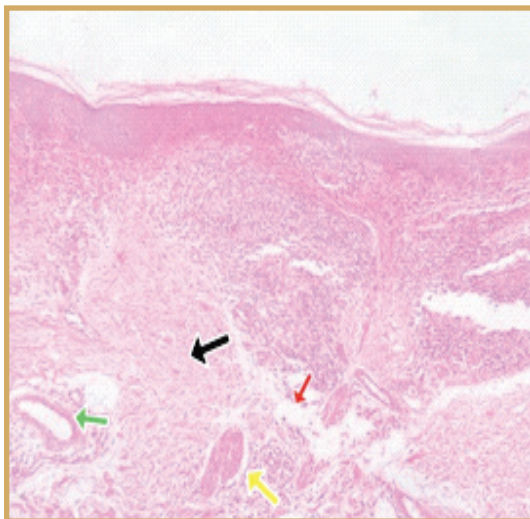
Fig. 8 (a-d): Type 1 reaction. (a) Single, erythematous and edematous plaque over abdomen. **(b)** On dermoscopy of the affected area, intense erythema, white structureless areas (black arrows) and scaling (yellow arrows) are noted (DermLite DL3, magnification $\times 10$). **(c)** Telangiectatic vessels (black arrows), follicular plugging (white arrow) (DermLite DL3, magnification $\times 10$). **(d)** Histopathology showing orthokeratosis (red arrow), dermal edema (black arrow) with deep dermis and subcutis shows lymphohistiocytic collections (yellow arrow) along with giant cells (H&E, $\times 10$).



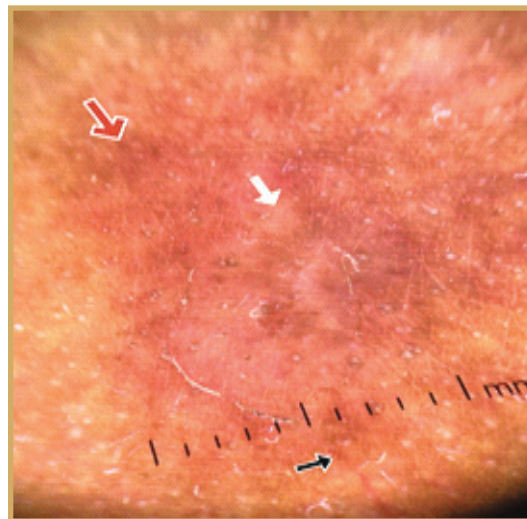
9a



9b



9d



9c

Fig. 9 (a-d): Type 2 reaction. (a) Multiple erythematous plaques over bilateral upper limbs. (b) On dermoscopy of the affected area, central yellowish brown structureless area (red arrows) with peripheral erythema and pigmentation (black arrows) giving rise to targetoid appearance (DermLite DL3, magnification $\times 10$). (c) Telangiectatic vessels (black arrows), white structureless areas (white arrows), erythema (red arrows) (DermLite DL3, magnification $\times 10$). (d) Histopathology showing dermal edema (red arrow), fibrosis (black arrow), peri-adnexal and perivascular infiltrates of lymphocytes, histiocytes, epithelioid histiocytes (green arrow) and hypertrophied nerve bundles (yellow arrow). Subcutis shows perivascular infiltration of acute and chronic inflammatory cells (H&E, $\times 40$).

Table 1 : Correlation of dermoscopy and histopathology findings.

Dermoscopic features	Correlating with histopathological findings
Structureless areas White structureless areas Yellowish brown structureless areas	Dermal granuloma
Decreased appendages	Peri-appendageal granuloma Peri-appendageal inflammatory infiltrate
Telangiectasia Diffuse erythema Peripheral erythema	Perivascular inflammatory infiltrate Dilated blood vessels Perivascular granuloma
Scaling	Hyperkeratosis
Follicular plugging	Hyperkeratosis
Xerosis	Hyperkeratosis
Chrysalis-like structures	Dermal fibrosis
Patchy areas of reduced pigmentary network	Damage to melanocytes in basal layer
Accentuation of pigment network	Increased basal layer pigmentation

examination revealed patchy loss of pigment network in all 3 patients (100%), with sparing of appendages (Fig. 6b). Perivascular and periadnexal lymphohistiocytic cells were noted in the histopathological evaluation (Fig. 6c).

Histoid leprosy cases displayed a unique clinical presentation of multiple, umbilicated, skin-colored papules and nodules (Fig. 7a). Dermoscopy of lesions had a sunflower-like appearance with petal-like configuration of white areas (n=3,100%), perilesional hyperpigmentation (n=3,100%), and crown blood vessels (n=3,100%) (Fig. 7b). A central keratotic plug corresponding to umbilication was also noted in one patient (Fig.7c). Histopathology revealed expansile granuloma with spindle-shaped cells and upward displacement of dilated vessels by dermal granuloma (Fig. 7d). The presence of dermal fibrosis in histopathology can be correlated to the shiny white areas seen in dermoscopy.

Patients with type 1 reaction presented with erythematous and oedematous plaques (Fig.

8a). Dermoscopy exhibited intense erythema in all patients (n=13, 100%) along with scaling (n=9, 69.2%), telangiectasia (n=8, 61.5%), and follicular plugging (n=5, 38.56%) (Figs. 8b, 8c). Histopathological examination revealed hyperkeratosis, inflammatory infiltration and dilated blood vessels (Fig. 8d), which are consistent with the dermoscopic findings.

Patients with type 2 reaction presented with multiple, evanescent, erythematous, tender nodules over limbs (Fig. 9a). Erythema (n=12, 100%) and vascular dilatation (n=8, 66.6%) were noted in dermoscopic evaluation (Figs 9b, 9c). A peculiar finding of central white chrysalis-like structure with peripheral erythema giving rise to a targetoid appearance was seen in 10 (83.33%) patients with type 2 reaction (Fig. 9d). The central whitish to violaceous structureless area can be correlated histologically to granulomatous infiltrate, chrysalis-like whitish streaks to dermal fibrosis, and peripheral erythema to perivascular inflammation and increased vascularity. Branching blood vessels were consistently seen

against a backdrop of hyperpigmentation in dermoscopy.

Discussion

The categorization of leprosy can often be challenging due to atypical and overlapping manifestations across its spectrum mainly on account of changing immune status of person with respect to leprosy. Invasive tools such as histopathological analysis is often essential. A non-invasive, innovative modality such as dermoscopy can help in identifying various dermatoses and the same can be used for aiding in categorization.

Yellowish orange structureless areas are hallmark dermoscopic findings of granulomatous disorders. This is due to the mass effect caused by dermal granulomas and inflammation. These findings are better seen by blanching the vessels through application of pressure. The presence of vascular structures can be explained by the pressure exerted by the granuloma, pushing the dilated vessels upwards (Bombonato et al 2015, Errichetti & Stinco 2018). Dermoscopic findings are also influenced by the stage of the disease and level of infiltration. Early lesions and deeper infiltration may fail to yield the characteristic yellow structureless areas in dermoscopic examination (Bombonato et al 2015).

We have compared our dermoscopic observations and corresponding histological features and were able to correlate them, as depicted in Table 1. White structureless areas, chrysalis-like streaks, variable loss of appendageal structures, yellowish-brown structureless areas were predominant features observed in this study throughout the spectrum. Yellowish brown and white structureless areas correlate with dermal granulomas whereas the chrysalis like streaks occur secondary to dermal fibrosis. Perivascular and periappendageal granulomas were noted histologically in lesions with sparse skin appendages and an erythematous hue. The

presence of loss of pigment network can be attributed to fewer melanocytes in the affected patches of leprosy.

Similar studies have been conducted by Agharia et al (2023), Mohta et al (2021), Chopra et al (2019), Ankad et al (2024) and Vinay et al (2019) on 50, 73, 50, 53 and 30 patients, respectively. Vinay et al (2019) and Chopra et al (2019) observed yellowish orange areas with vascular abnormalities and absence of skin appendages consistently throughout the spectrum meanwhile distorted pigment network was the most common finding observed by Ankad et al (2024). Instead of the yellowish orange structureless area seen in earlier studies (Agharia et al 2023, Chopra et al 2019, Vinay et al 2019), we found that in the majority of our cases, yellowish-brown structureless areas were observed. This can be attributed to the skin phototype being Fitzpatrick type IV to VI. Decreased pigmentation with white structureless areas and variable loss of skin appendages were noted by us in all spectrums of leprosy without reaction, which are consistent with observations made by Chopra et al (2019) and Mohta et al (2021). Scaling, white structureless areas, yellowish brown structureless areas were seen more commonly in the tuberculoid spectrum in this study. This observation reinforces the findings noted by previous studies. We recorded chrysalis like streaks and patchy accentuation of reticular pigment predominantly in patients with borderline lepromatous and lepromatous leprosy, similar to the findings noted by Ankad et al (2024), Mohta et al (2021) and Vinay et al (2019). On the other hand, Agharia et al (2023) observed patchy loss of pigment network in lepromatous pole. This disparity could be due to increased incidence of repeated reactions among patients included in our study.

Branching blood vessels were seen in this study in patients in reaction and in patients with Histoid

Hansen. Violaceous structureless areas with large branching blood vessels, intense erythema, follicular plugging and scaling were novel findings noted in type 1 reaction. A similar observation was noted in patients in type 1 reaction by Vinay et al (2019) and Ankad et al (2024). We noted a unique targetoid pattern in type 2 reaction with central structureless area and peripheral erythema. Similar findings were also observed in a study done by Agharia et al (2023) on 50 leprosy patients. In the case of histoid leprosy, a characteristic petal like arrangement of white areas with crown vessels were seen. We didn't observe the yellowish-orange structureless area and milky white pink background in histoid Hansen as noted by Vinay et al (2019), Ankad et al (2024), Agharia et al (2023) in their studies. Whorled configuration of spindle shaped cells in histoid Hansen is most likely the cause of white areas noted in this study.

Along with the characteristic yellowish orange globules seen in granulomatous disorders, the presence of decreased white dots (absence of sweat duct openings), decreased hair follicles, focal loss of pigment network, chrysalis like streaks and branching blood vessels can help physicians differentiate leprosy from other granulomatous disorders. Moreover, the presence of erythema, telangiectasia, follicular plugging can aid in the diagnosis of reactions in leprosy (Jha et al 2020). Early diagnosis and treatment of reaction can prevent disabilities and deformities in leprosy patients and thus help in improving their quality of life.

The distinctive feature of our study, as compared to earlier research, is the correlation between dermoscopic results and histological characteristics of all types of leprosy. The major dermoscopic features of atypical types of leprosy, including indeterminate, histoid Hansen and lepra reactions have been documented in

this study. We were able to observe significant dermoscopic changes and establish an obvious correlation with the histopathological changes in our study population. Dermoscopy has an immense amount of potential as a diagnostic tool especially in situations where an invasive test like biopsy is not preferred. Dermoscopy provides an additional advantage of being rapid, can be performed at the point of care, does not require time for processing and interpretation.

References

1. Acharya P, Mathur MC (2020). Clinicodermoscopic study of histoid leprosy: A case series. *Int J Dermatol*. **59** (3): 365-368.
2. Agharia RS, Mehta HH, Bharti A et al (2023). Dermoscopic, clinical, and histopathological aspects of leprosy and lepra reaction cases: An observational cross-sectional study. *Indian J Dermatopath Diagn Dermatol*. **10**(1): 1-11, | doi: 10.4103/ijdpdd.ijdpdd_3_22.
3. Ankad BS, Sharma A, Vinay K et al (2024). Dermatoscopic evaluation of leprosy: A multi-centre cross-sectional study. *Indian J Dermatol Venereol Leprol*. **90**(4):486-493. doi: 10.25259/IJDVL_506_2023.
4. Bombonato C, Argenziano G, Lallas A et al (2015). Orange color: a dermoscopic clue for the diagnosis of granulomatous skin diseases. *J Am Acad Dermatol*. **72**(1): S60-S63.
5. Chopra A, Mitra D, Agarwal R et al (2019). Correlation of dermoscopic and histopathologic patterns in leprosy – A pilot study. *Indian Dermatol Online J*. **10**(6): 663-668.
6. Errichetti E, Stinco G (2018). Dermatoscopy of granulomatous disorders. *Dermatol Clin*. **36**(4): 369-375. doi: 10.1016/j.det.2018.05.004.
7. Indian Association of Leprologists (1982). Clinical, histopathological, and immunological features of the five-type classification approved by the Indian association of leprologists. *Lepr India*. **52**: 22–32.
8. Jha AK, Zeeshan MD, Tiwary P et al. (2020). Dermoscopy of type 1 lepra reaction in skin of color. *Dermatol Pract Conceptual*. **10**(3): e2020083. Doi: 10.5826/dpc.1003a83.

9. Kar HK, Gupta R (2016). Management of leprosy reactions. In: IAL Textbook of Leprosy, 2nd Edition, (Bhushan Kumar, Kar HK, Eds), Jaypee Brothers Medical Publishers (P) Ltd, Delhi, pp 465-477.
10. Mohta A, Jain SK, Agrawal A et al (2021). Dermoscopy in leprosy: A clinical and histopathological correlation study. *Dermatol Pract Concept*. **11(2)**: e2021032. doi: 10.5826/dpc.1102a32.
11. Ridley DS, Jopling WH (1966). Classification of leprosy according to immunity. A five-group system. *Int J Lepr Other Mycobact Dis*. **34**: 255–273.
12. Sardana K (2020). The disease. In: Jopling's Handbook of Leprosy, 6th edition, (Sardana K, Khurana A, Eds), CBS Publishers & Distributors Private Limited, pp 6-9.
13. Sonthalia S, Pasquali P, Agrawal M et al (2019). Dermoscopy update: review of its extradiagnostic and expanding indications and future prospects. *Dermatol Pract Concept*. **9(4)**: 253-264. doi:10.5826/dpc.0904a02.
14. Vinay K, Kamat D, Chatterjee D et al (2019). Dermoscopy in leprosy and its correlation with clinical spectrum and histopathology: a prospective observational study. *J Eur Acad Dermatol Venereol*. **33(10)**: 1947-1951. doi: 10.1111/jdv.15635.

How to cite this article : Sameeha HC, Sravani K, Divya B et al (2024). Correlation of Dermatoscopic Findings in Leprosy with Clinical Spectrum and Histopathology: A Prospective Observational Study. *Indian J Lepr*. **96**: 215-230.